BRL

REPORT No. 1009

MARCH 1957

An Application Of Nonlinear Theory To The Yawing Motion Of Mortar Shell

INGEBORG B. KISTLER

DEPARTMENT OF THE ARMY PROJECT No. 5B03-03-001
ORDNANCE RESEARCH AND DEVELOPMENT PROJECT No. TB3-0108

BALLISTIC RESEARCH LABORATORIES

ABERDEEN PROVING GROUND, MARYLAND

Destroy when no longer needed. DO NOT RETURN

B A L L I S T I C R E S E A R C H L A B O R A T O R I E S

REPORT NO. 1009

MARCH 1957

AN APPLICATION OF NONLINEAR THEORY TO THE YAWING MOTION OF MORTAR SHELL

Ingeborg B. Kistler

Department of the Army Project No. 5B03-03-001
Ordnance Research and Development Project No. TB3-0108

A B E R D E E N P R O V I N G G R O U N D, M A R Y L A N D

TABLE OF CONTENTS

B A L L I S T I C R E S E A R C H L A B O R A T O R I E S

REPORT NO. 1009

IBKistler/cer
Aberdeen Proving Ground, Md.
March 1957

AN APPLICATION OF NONLINEAR THEORY TO THE YAWING MOTION OF MORTAR SHELL

ABSTRACT

The results of C. H. Murphy's analysis of the nonlinear yaw equation are applied to the specific case of the 81-mm M56 shell. By means of this example a general method of analysing and predicting the motion of fin stabilized projectiles is developed; the method permits spin variation to be included in the analysis. It is believed that this study can be a guide to new experimental work on the phenomenon of short ranges of mortar fire and that it can be an aid in the interpretation of experimental data.

TABLE OF SYMBOLS

A		axial moment of inertia
B		transverse moment of inertia
d		diameter
g		acceleration of gravity
H	$=$	$J_L - J_D + k_2^{-2} J_H$
J_i	$=$	$\frac{\rho d^3}{m} K_i \quad i = D, H, L, M, T$
J_g	$=$	$-\frac{g \sin \delta \, d}{u^2}$
K_D		drag coefficient
K_H		moment coefficient due to cross angular velocity
K_L		lift force coefficient due to yaw
K_M		moment coefficient due to yaw
K_T		Magnus moment coefficient
K_i	$i=1,2$	amplitude of the i-th frequency
k_1		axial radius of gyration
k_2		transverse radius of gyration
ℓ		cosine of the angle of yaw
m		mass
M	$=$	$k_2^{-2} \quad J_M$
S		surface generated by separatrices
T	$=$	$J_L - k_1^{-2} J_T$
u		magnitude of velocity
α		logarithmic rate of growth of yaw (pure mode motion)
α_1		logarithmic rate of growth of nutation
α_2		logarithmic rate of growth of precession

α_{ij}	i=1,2; j=0,2,4 coefficients in equations (6) and (7)
δ	angle of yaw, also sine of angle of yaw
θ	angle between separatrix and K_1^2 - axis at the saddle point
λ	complex yaw
ν	spin in radians per caliber
ν_1	lower limit of spin for instability
$\bar{\nu}$	$\frac{A}{B}\ \nu$
ρ	density
$\tilde{\phi}_i$ i=1,2	phase angle of the i-th frequency in the solution of the linearized equation.
ψ_i i=1,2	parametric functions for frequency correction
$(\ )_o$	initial conditions.

INTENTIONALLY LEFT BLANK.

I. INTRODUCTION

The work discussed in this report was undertaken in an effort to clarify the problem of short ranges of mortar fire. It turns out that about two out of one hundred rounds reach considerably less than the expected range. This short round behavior has been of general concern for some time since it endangers friendly troops.

The immediate cause for short rounds is the development of large angles of yaw. This occasional growth of yaw cannot be explained by linear theory. It has, therefore, been suggested that these fin-stabilized projectiles are spinning, even when the fins are not canted, (Ref. 1) and subsequent measurements showed that the resulting Magnus torque is nonlinear with respect to spin and yaw (Ref. 2).

There are then two aspects of the problem which have to be investigated: 1) the generation of spin and 2) the effect of spin on yaw. The latter aspect of the problem is treated in this report for the particular case of the 81-mm M56 shell. The method used here can, however, be applied to any shell.

As a result of the present analysis it will be possible to determine the combinations of values of yaw and spin which will result in large yawing motion. In addition, the results enable one to obtain an estimate of the spin generation which can produce these unstable conditions.

II. SPIRAL YAWING MOTION

The hypothesis that spin may be one of the phenomena explaining short ranges was stated by Zaroodny as early as 1946. (Ref. 3) The most convincing evidence in support of this theory was the wind tunnel measurements of the Magnus torque of the 81-mm M56 shell reported in BRL Report No. 882 by Zaroodny and Mott. These measurements show that

the Magnus torque is highly nonlinear with respect to both spin and yaw, and that the linearized theory of the yawing motion is applicable only up to about 2° of yaw, and not up to some 10° as had been believed (Ref. 2). The Magnus torque coefficient, K_T, was found to be approximated by the expression (Ref. 4),

$$\begin{aligned} K_T &= K_{T_{00}} + K_{T_{02}} \nu^2 + K_{T_{04}} \nu^4 \\ &+ (K_{T_{20}} + K_{T_{22}} \nu^2 + K_{T_{24}} \nu^4) \delta^2 \\ &+ (K_{T_{40}} + K_{T_{42}} \nu^2 + K_{T_{44}} \nu^4) \delta^4 \end{aligned} \qquad (1)$$

where

ν = spin in radians per calibers

δ = angle of yaw in radians

It follows from these findings that the effect of spin on yaw cannot be neglected, and that, furthermore, the nonlinear form of the Magnus torque coefficient, equation (1), should be introduced into the equation of yaw.

An approximate solution to the nonlinear yaw equation was obtained by Zaroodny and Bomberger for the special case of constant spin and spiral yawing (Ref. 4). The present report is essentially an extension of their work for the more general case of epicyclic yawing motion.

Considering the two types of spiral yawing, pure precession and pure nutation, at various values of spin, Zaroodny and Bomberger found the two essentially different solutions which are shown in Figures 1 and 2. The curves drawn in the two figures are the loci of the angles of yaw which remain constant. They are the curves of zero damping. For pure precession (Fig. 1) no development of large angles of yaw occurs. The curve $\alpha = 0$ is the locus of a stable equilibrium of circular precession. Points to the right of this curve represent combinations of yaw and spin which result in a decrease in yaw. Points to the left correspond to conditions of growing yaw. Zero yaw appears to be an unstable condition for values

of spin above a certain minimum, about $\nu = .045$, given by the intersection of the $\alpha = 0$ curve and the spin axis. For pure nutation (Fig. 2) large angles of yaw will develop of the initial values if spin and yaw are large enough. The curve $\alpha = 0$ is here the locus of an unstable equilibrium of circular nutation. Small initial yaws, represented by points to the left of the curve, will shrink to zero, and zero yaw is a stable condition. At points to the right of the curve the yaw will grow. The horizontal arrows represent the directions of the trajectories of the yawing motion for constant spin.

Looking at these results in a plot of precession against nutation for a constant value of spin (Fig. 3), one observes that the yawing motion is determined by three singularities. For the particular spin of $\nu = .1$ rad/caliber there are: an unstable equilibrium of circular nutation at about 13°, the origin, and a stable equilibrium of circular precession at about 7.5°. The arrows again indicate the direction of the possible trajectories. The nutational yawing motion will grow for angles larger than 13°, it will shrink to zero for smaller angles. At zero yaw the precession appears to be building up resulting in a limit motion of circular precession at 7.5°. For angles larger than 7.5° the precession decreases and the same limit motion results. How the precession can build up starting from zero yaw is a puzzling question which cannot be answered by this analysis. What is happening will, however, become clear when the general epicyclic motion is discussed.

III. EPICYCLIC YAWING MOTION

The yawing motion along the two axes in Figure 3 is well determined by the analysis of Reference 4, but the actual yawing motion of shell will not necessarily begin at a point where one of the two amplitudes is zero. The trajectory describing the yawing motion will in general be a curve that can start anywhere in the plane of Figure 3. Extrapolating from the yawing motion on the axes, it seems reasonable to expect that there

will exist a curve separating initial conditions leading to zero or small yaw limit motions from those resulting in large yaws. This curve should go into the point of unstable equilibrium on the nutational axis. In order to obtain qualitative results for the general yawing motion in this plane, and similar planes for different values of spin, the results of C. H. Murphy's treatment of the nonlinear yaw equation were applied (Ref. 5).

Three basic assumptions have been made in the following analysis. (1) The effects of any asymmetry and of the yaw of repose have been neglected. (2) The instantaneous yawing motion is considered to be a function of spin but not of the rate of change of spin. (3) The spin and the amplitude of yaw are assumed to change little over a period of yaw. (A factor of 2 in the maximum amplitude is believed to be tolerable.) With these assumptions the results of BRL Report 995 can be applied directly to the yawing motion of the 81-mm M56 shell for various values of spin.

Neglecting the effect of gravity ($J_g = 0$), letting $\ell \doteq 1$, $\delta \doteq \sin \delta$* and otherwise using the aerodynamic coefficients given in the appendix of Reference 4, one can write equation (41) of Reference 5 in the simplified form,

$$\lambda'' + (H - i\bar{\nu})\,\lambda' - (M + i\,\bar{\nu}\,T)\,\lambda = 0 \qquad (2)$$

where $H = J_L - J_D + k_2^{-2}\,J_H$

$\bar{\nu} = \frac{A}{B}\,\nu$

$M = k_2^{-2}\,J_M$

$T = J_L - k_1^{-2}\,J_T$

and $J_i = \frac{\rho d^3}{m}\,K_i$

(For definitions consult the Table of Symbols.)

* From here on δ will be used to denote the sine of the angle of yaw.

The aerodynamic coefficients J_i are constant with the exception of the Magnus torque coefficient, J_T. J_T is given by the expression of equation(1),and for any particular value of spin the Magnus torque coefficient is of the form,

$$J_{T_0} + J_{T_2} \delta^2 + J_{T_4} \delta^4$$

The solution of equation 2 is then assumed to be,

$$\lambda = K_i e^{i(\psi_1 + \tilde{\phi}_1)} + K_2 e^{i(\psi_2 + \tilde{\phi}_2)} \tag{3}$$

(Equation(26)of Reference 5) where $\tilde{\phi}_1$ and $\tilde{\phi}_2$ are the phase angles occurring in the solution to the linearized equation but K_i and ψ_i are unknown functions of p. By the method of Kryloff and Bogoluiboff approximate solutions of K_i and ψ_i can be found. For this particular case the solutions for the amplitudes are given by equations (49) and (50) of Reference 5.

$$\frac{(K_1^2)'}{K_1^2} = -2\alpha_1 \tag{4}$$

$$\frac{(K_2^2)'}{K_2^2} = -2\alpha_2 \tag{5}$$

where

$$\alpha_1 = \alpha_{10} + \alpha_{12}(\delta^2)_{e_1} + \alpha_{14}(\delta^4)_{e_1} = \frac{H\tilde{\phi}_1' - \bar{\nu}\left[T_0 + T_2(\delta^2)_{e_1} + T_4(\delta^4)_{e_1}\right]}{\tilde{\phi}_1' - \tilde{\phi}_2'} \tag{6}$$

$$\alpha_2 = \alpha_{20} + \alpha_{22}(\delta^2)_{e_2} + \alpha_{24}(\delta^4)_{e_2} = \frac{H\tilde{\phi}_2' - \bar{\nu}\left[T_0 + T_2(\delta^2)_{e_2} + T_4(\delta^4)_{e_2}\right]}{\tilde{\phi}_2' - \tilde{\phi}_1'} \tag{7}$$

and

$$(\delta^2)_{e_1} = K_1^2 + 2K_2^2 \quad , \quad (\delta^2)_{e_2} = K_2^2 + 2K_1^2$$

$$(\delta^4)_{e_1} = K_1^4 + 6K_1^2 K_2^2 + 3K_2^4, \quad (\delta^4)_{e_2} = K_2^4 + 6K_1^2 K_2^2 + 3K_1^4$$

The effective values of δ^2 and δ^4 are obtained by the averaging process of the K-B method, and they represent the essential difference between the nonlinear and the linear solution.

Murphy then found it convenient to study the yawing motion in terms of K_1^2 and K_2^2, the squares of the sines of the nutational and precessional angles of yaw, rather than the angles of yaw directly. If the scales along the two axes in Figure 3 are changed accordingly, the resulting plane is what Murphy calls the "amplitude plane". Only the first quadrant of this plane is of interest since the squared amplitudes are always positive. The equation determining the trajectories of the yawing motion in this plane follows directly from equations (4) and (5). (Equation 57 of Ref. 5)

$$\frac{d(K_2^2)}{d(K_1^2)} = \frac{K_2^2 \alpha_2}{K_1^2 \alpha_1} \tag{8}$$

A certain amount of information is known about the trajectories before equation (8) is actually solved. It is known, for instance, that the trajectories have to cross the $\alpha_1 = 0$ curve with a vertical, the $\alpha_2 = 0$ curve with a horizontal slope. The zero damping curves are hyperbolas for the present case. The coefficients α_{ij} $(i=1,2;\ j=0,2,4)$ in equations (6) and (7) are functions of the spin ν. As the spin is changed the centers of the hyperbolas shift slightly along straight lines. The centers of $\alpha_1 = 0$ are located along the line $K_1^2 = 3K_2^2$, the centers of $\alpha_2 = 0$ on $K_2^2 = 3K_1^2$. The slopes of the asymptotes of both families of hyperbolas remain constant as the spin is changed, but the length of the transverse axes is changing, and for the $\alpha_1 = 0$ family it even goes through zero resulting in an interchange of the transverse and conjugate axes. (See in particular Figures 6 and 7).

More important than the zero damping curves are the singularities of equation (8) in determining the motion of the shell. The singularities of equation (8) are given by the following four pairs of equations:

(a) $K_1^2 = 0$ $K_2^2 = 0$

(b) $K_1^2 = 0$ $\alpha_2 = 0$

(c) $K_2^2 = 0$ $\alpha_1 = 0$

(d) $\alpha_1 = 0$ $\alpha_2 = 0$

Singularities given by the first three pairs of equations can be found by the method of Zaroodny and Bomberger. They are (a) the origin, (b) singularities on the precessional axis, (c) singularities on the nutational axis. The fourth pair of equations determines singularities which cannot be found by the earlier method, limit epicycles. When the zero damping curves are hyperbolas there can be as few as one and as many as seven singularities in the first quadrant. In this particular case, the number of singularities increases from two to seven with an increase in spin. They are of only three different types: stable nodes, saddle points, and stable spirals; the first two types occur on the axes, the latter correspond to the limit epicycles.

Besides zero damping curves and singularities there is a third factor determining the shapes of the trajectories. As mentioned above, there should be a curve going into a saddle point, the unstable equilibrium, which separates trajectories turning to one or the other side of the saddle. Such a curve is called a separatrix, and it is the only trajectory going into or coming out of a saddle. The separatrices are not defined by simple algebraic equations and hence cannot be determined in advance of an actual solution of equation (8).

Equation (8), the differential equation determining the trajectories in the amplitude plane, was solved by a GEDA (Goodyear Electronic Differential Analyser) model GN 215-23. The machine's output can be automatically recorded on a large plotting board giving one variable as a function of the other. In this way the amplitude planes shown in Figures 4 through 10 were actually drawn by the GEDA. In the neighborhood of the axes and the zero damping curves the accuracy of these figures is relatively poor.

The multipliers of the machine have a constant error of .2 volts, so that the products of very small numbers have high percentage errors. In order to show the complete region of interest, including the large yaw limit motions, accuracy had to be sacrificed. By rescaling the problem and solving for a small portion of the amplitude planes at a time one can, however, obtain the solutions to the desired degree of accuracy.

A short description of GEDA is found in Ref. (6). For a more detailed report on the machine see Ref. (7).

By means of the GEDA the determination of the separatrices is very simple. Initial conditions have to be chosen in such a way that the separatrix is approached from both sides. This process will quickly give two trajectories which lie close together and run parallel up to the saddle point but separate there. The separatrix can then be drawn between them.

The data upon which the expression for K_T is based go only up to a maximum of yaw of about 20^o. The curve of 20^o of maximum of yaw is shown in Figure 12. The parts of the trajectories beyond this curve are based on an extrapolation of the expression for K_T to larger angles. While one cannot assume these parts of the trajectories to be exact, one can assume that they give a qualitative picture of the yawing motion at these large angles. The complete plots of the amplitude planes can then serve as an aid for planning new experiments as well as for interpreting experimental results. Recent experiments reported in Reference (9) can quite possible be explained by means of these plots, and can be considered to justify the above statements about the extrapolation to large angles of yaw.

IV. AMPLITUDE PLANE ANALYSIS FOR CONSTANT SPIN

The lowest spin considered in the analysis is $\nu = .025$ (Figure 4). At this spin only one branch of each zero-damping hyperbola is present in the first quadrant. The $\alpha_2 = 0$ branch intersects the K_2^2 - axis at $K_2^2 = .2836$, and there is a saddle point of about 32° precession. The region beyond the separatrix is definitely outside the region of interest, and this separatrix (which does not change much as the spin increased) is not shown in the following figures. The $\alpha_1 = 0$ branch does not intersect the K_1^2 - axis, so that there are no singularities on the nutational axis. The origin is a stable node.

For the next spin, $\nu = .035$ (Figure 5), both branches of $\alpha_1 = 0$ are in the first quadrant, resulting in two singularities on the nutational axis. The one closest to the origin is a saddle, the other one a node. Trajectories starting to the right and below the separatrix end in a limit motion of circular nutation. Only a very small region of the amplitude plane constitutes this unstable region. Otherwise there is little change from the amplitude plane for $\nu = .025$.

At a spin of $\nu = .045$ (Figure 6) the second branch of the $\alpha_2 = 0$ hyperbola has moved into the first quadrant, but it is still so close to the origin that it cannot be seen. Similarly, the two right branches of the two hyperbolas do now have an intersection in the first quadrant, which is so close to the nutational axis that the singularity still appears to lie on the axis.

As the spin varies from $\nu = .045$ to $\nu = .05$ the transverse axis of the $\alpha_1 = 0$ hyperbola goes through zero and at $\nu = .05$ (Figure 7) the hyperbola has moved to the other side of the asymptotes. The intersection of the right branches of the two hyperbolas is here far enough removed from the axis to reveal that it is a limit epicycle and a spiral point, and that both singularities on the nutational axis are now saddles. The left branch of the $\alpha_2 = 0$ curve is now also far enough away from the origin

to be discerned, and it is clear that the origin is now a saddle while the intersection of the left branch of $\alpha_2 = 0$ with the K_2^2 -axis defines a stable node of circular precession in agreement with Figure 1. This one and the following figures explain the build up of precession, so puzzling when only spiral yawing motion is considered. What happens is this: the nutation does not become zero until the node on the precessional axis is reached, and the precession begins to build up starting from a small but non-zero value of precession.

The next two figures (Figures 8 and 9) for values of spin $\nu = .1$ and $\nu = .15$ show on the whole only quantitative changes. The saddle defined by the left branch of $\alpha_1 = 0$ and the nutational axis is coming closer to the origin, the angle of the node of circular precession is increasing, and the limit epicycle is moving farther away from the nutational axis and coming closer to the precessional axis.

The last of this series of plots for a spin of $\nu = .25$ (Figure 10) shows one additional qualitative change since here the left branches of the two hyperbolas intersect in the first quadrant. The stable node on the precessional axis has become a saddle point and the limit motion for the stable case is now also a limit epicycle.

With these amplitude planes it is possible to predict the yawing motion of a shell for constant spin if the initial components of precession and nutation are given. The initial phase does not have to be known.

V. EFFECT OF SPIN VARIATION ON THE YAWING MOTION

The results of the preceding chapter indicate which angles of yaw can produce short rounds at given values of spin. However, since shell are extremely unlikely to have initial values of spin and yaw of the amount necessary to produce large yawing motion directly, an attempt was made to include the effects of spin generation by analysing the complete set of

amplitude planes simultaneously. This can be done provided the spin varies slowly enough so that the amplitude planes for constant spin do represent the instantaneous situation.

The type of analysis intended can be simply illustrated for the spiral yawing motion. Let initial conditions (δ_0, ν_0) be given on the stable side of the zero damping curve (Figure 11). On this side the yaw is decreasing, and, for constant spin, the trajectory is represented by a horizontal line directed to the left. If the spin is increasing the trajectory will be bent upward. In the extreme case, where the spin increases much faster than the yaw, the trajectory will approach a vertical line directed upward, but as long as it is on the left side of the $\alpha = 0$ curve it cannot go to the right. Hence, the intersection of the vertical line through the initial point, $\delta = \delta_0$, and the curve of zero damping, $\alpha = 0$, will define a lower limit of spin, ν_1 , which can possibly produce large yawing motion; i.e., if the spin varies only between zero and ν_1, and does not exceed ν_1, the yawing motion will certainly be stable.*

For the three-dimensional trajectories - precession, nutation, and spin varying - the analysis is complicated by the fact that the slope of the trajectory at a point in the amplitude plane is a function of all three variables. For spiral yawing it was sufficient to give the initial angle of nutation for the determination of the lower limit of spin needed for the development of large yaws. One would hope then, that it might be possible to determine such a limit of spin for the epicyclic yawing motion if the initial precession and nutation are given. Since points along the curve of Figure 11 correspond to the separatrices of Figures 4 through 10, the curve $\alpha(\delta, \nu) = 0$ itself will correspond to a surface $S(K_1^2, K_2^2, \nu) = 0$ generated by the separatrices; as the equation $\alpha(\delta_0, \nu) = 0$ gave the lower limit of spin, ν_1, for the case of spiral yawing, it is hoped that the

---

* Zaroodny showed in Reference 8 that the spin variation is usually so slow that the $\alpha = 0$ curve is a close approximation to the curve separating stable from unstable initial conditions when the spin is allowed to vary.

relation $S(K_{10}^2, K_{20}^2, \nu) = 0$, defining a point on the surface, will determine the lower limit ν_1 for the epicyclic motion.

Figure 12 shows the separatrices for various values of spin. In relation to the surface S these curves represent contour lines whose heights are given by the values ν. The value ν_1 given by the equation $S(K_{10}^2, K_{20}^1, \nu) = 0$ is the spin whose separatrix goes through the initial point in Figure 12. However, for this spin to be the desired lower limit, all trajectories with values of spin less than ν_1 have to move to the left of the separatrix for ν_1 at that point, i.e., the slope of the trajectory given by equation (8) if it is evaluated at $(K_{10}^2, K_{20}^2, \nu)$ with $\nu < \nu_1$, has to be smaller than the slope of the separatrix for ν_1 at the point (K_{10}^2, K_{20}^2).

It will now be necessary to investigate whether the relation between the slopes of the low spin trajectories and the higher spin separatrix through the same point does hold everywhere to the left of the corresponding low spin separatrices in the plane of Figure 12, or, if not, whether it holds in the region of interest.

An inspection of Figure 12 reveals that an increase in spin shifts the descending parts of the separatrices to the left and raises the value of the maximum. Furthermore, the angle, θ, between the separatrices and the nutational axis at the saddle points increases for increasing spin. As mentioned before, the plots are not very accurate in the neighborhood of the zero-damping curves. Therefore, a list of the theoretical values of these angles follows. The angles were determined with the equation,

$$\lim_{\substack{K_2^2 \longrightarrow 0 \\ \alpha_1 \longrightarrow 0}} \frac{d(K_2^2)}{d(K_1^2)} = \frac{\alpha_{20} + 2\alpha_{22} K_1^2 + 3\alpha_{24} K_1^4}{2\alpha_{12} K_1^2 + 6\alpha_{14} K_1^4} \quad . \qquad (10)$$

ν	.035	.045	.05	1	.15	.25
tan θ	1.313	-9.582	-4.128	-1.389	-1.133	-.9837
θ	$52^\circ\ 42'$	$95^\circ\ 58'$	$103^\circ 37'$	$125^\circ 45'$	$131^\circ 26'$	$134^\circ 32'$

Since the angle between the separatrix and the horizontal increases with increasing spin for $K_2^2 = 0$, the same will be true for $K_2^2 > 0$ up to a certain value of K_2^2. The graph indicates this fact in that the horizontal distances between the descending branches of the various separatrices do not decrease as K_2^2 is increased, and, in fact, these distances do not seem to decrease until the separatrices reach their maxima. A theoretical justification for this observation, although no proof, is the fact that a low spin separatrix has both its vertical and its horizontal slopes at a smaller value of K_2^2 than a higher spin separatrix.

Besides the relation between the various separatrices, the relation between each separatrix and its trajectories is needed. Studying the Figures 4 through 10 in the order of increasing spin and observing in particular the trajectories leading to zero or small yaw limit motions (the only ones for which the concept of a lower limit of spin is meaningful) one can find a relation between the slopes of the trajectories and the slopes of the separatrix.

The lowest spin for which a separatrix comes into the nutational axis is $\nu = .035$. This separatrix has a positive slope at the saddle and the trajectories to its left have positive slopes everywhere with the exception of the small region enclosed by the left branch of $\alpha_1 = 0$. The trajectories have to enter and leave this region with a vertical slope, and their directions inside differ only little from the vertical.

At a spin of $\nu = .045$ the separatrix has a negative slope at the saddle, and there exists a very small region to the left of the separatrix, inside the right branch of $\alpha_1 = 0$, where the slopes of the trajectories become negative, but again the angles with the horizontal increase only little above 90°. Outside this branch of $\alpha_1 = 0$ the situation is very much like that at a spin of $\nu = .035$, except that the region inside the left branch of $\alpha_1 = 0$ has become larger.

At a spin of $\nu = .05$ the hyperbola $\alpha_1 = 0$ has changed its position relative to the asymptotes and all the trajectories to the left of the

separatrix have to cross both its branches. The slope of the separatrix for this and the higher values of spin is negative everywhere between the nutational axis and the right branch of $\alpha_1 = 0$, while the trajectories have negative slopes between the two branches. This region between the two branches of $\alpha_1 = 0$ becomes larger as the spin is increased. In order to find out whether a trajectory will go to the left or the right of a separatrix which has negative slopes everywhere, one has to consider only those parts of the trajectories which have negative slopes since with a positive slope the trajectory will obviously not move to the right of its initial point, as long as only the descending parts of the trajectories are under consideration.

Crossing the left branch of $\alpha_1 = 0$ a trajectory has a vertical slope. At this value of K_2^2 the angle between the horizontal and this trajectory is certainly smaller than the angles between the horizontal and the trajectories farther to the right, including the separatrix. This same relation will hold for a certain region abovethis branch of the $\alpha_1 = 0$ curve. An approximate determination of the size of this region can be made by means of the graphs. It is known beforehand that the region will not go as far as the right branch of $\alpha_1 = 0$ since trajectories to the right of a given one will cross this branch (with a vertical slope) at smaller values of K_2^2 than trajectories to the left. Coming down from the right branch of $\alpha_1 = 0$ the trajectories on the left of the separatrix initially converge, then they diverge. The curve giving the points on the trajectories of shortest horizontal distance from the separatrix will limit the region in which the slope of the trajectories at a given value of K_2^2 decreases with distance from the separatrix. Below this curve the slope of the separatrix at a given value of K_2^2 can be considered as an upper limit of the slopes of the trajectories at the same value of K_2^2.

It was first shown that at a given value of K_2^2 the slopes of the separatrices increase with increasing spin. Then it was seen that in a certain region the slope of the separatrix is an upper limit of the

slopes of the trajectories for the same value of spin and at the same value of K_2^2. It follows that at a point in this same region the separatrix for a certain value of spin will have a larger slope than the trajectories for lower values of spin. It only remains to be determined if the region thus defined includes the region of likely initial conditions. The whole analysis is based on data going up to 20° of maximum of yaw, hence its validity for initial conditions outside this region is at least questionable. In addition, the shell are most likely to start out with almost planar yaw, which is represented by the 45° line in the amplitude plane. The curve of maximum yaw of 20° as shown in Figure 12 describes a region which appears to be well inside the region for which the above relations hold.

It can then be concluded that for any initial conditions to the right of the separatrix for the highest spin considered, there is a value of spin ν_1 given by the equation $S(K_{10}^2, K_{20}^2, \nu) = 0$ whose separatrix goes through the initial point. If the spin varies only between zero and this value, ν_1, the motion of the shell will certainly be stable. On the other hand, the spin has to increase at least beyond ν_1 for any large yawing motion to occur.

An illustration of the meaning of this analysis is included in Figure 12. For initial conditions of 20° precession, 20° nutation, and a spin of $\nu = .1$ the actual trajectory is shown. It is obvious that this trajectory goes to the left of the separatrix for $\nu_1 = .15$ which goes through the initial point.

It is possible to determine even more than this minimum value of spin necessary to produce large yawing motion. For given initial conditions one can determine the generation of spin necessary to account for large yaws. By determining the distance travelled by the shell while the trajectory in the amplitude plane reaches a certain separatrix (spin = ν_2) which was initially to its left, one can give an approximate value of the rate of change of spin needed if the shell is to acquire the spin ν_2 before the trajectory intersects this separatrix in Figure 12.

While the independent variable, distance in calibers of travel, has been eliminated in the equation for the trajectories, the speed of the pen of the GEDA is directly proportional to it. By introducing a mechanism which causes the pen to lift at equal time intervals, one can demonstrate the distance travelled by the shell, and the number of periods corresponding to a given piece of trajectory in the amplitude plane (Figure 13).

With reference to Figure 13 it must be pointed out that close to the singularities the pen is moving too slowly for the interruptions to be discernible. For large initial angles the pen is moving quite fast indicating rapid changes of yaw. A comparison with exact six degree of freedom trajectories computed on an electronic digital computer is planned in order to ascertain the limits of the approximations made in this analysis.

The trajectory shown in Figure 12 was transferred from Figure 13. One can see here that for an initial spin of $\nu_0 = .1$ and initial $K_{10}^2 = K_{20}^2 = .03$ the spin would have to reach the value $\nu_2 = .25$ in less than 3/5 of a period if that spin is to cause instability.

VI. CONCLUSION

The amplitude plane analysis used in this investigation represents a method for predicting the yawing motion of shell. In particular, this method, devised by C. H. Murphy and its adaptation for the case of variable spin allows one to determine the initial conditions of mortar fire which are likely to produce large angles of yaw and possibly short ranges. It also gives a means of estimating the rate of change of spin which would have to take place if spin generation is to explain the occurrence of short ranges.

ACKNOWLEDGMENT

The author is indebted to Mr. Serge J. Zaroodny who suggested and encouraged the work reported here.

She also wants to express her gratitude to Miss Betty Ann Hodes for her invaluable assistance throughout this investigation.

All the work on the analog computer was carried out by Mr. James W. Bradley and Mr. Donald C. Mylin.

Ingeborg B. Kistler

INGEBORG B. KISTLER

REFERENCES

(1) Zaroodny, Serge J., On the Mechanism of Dispersion and Short Ranges of Mortar Fire, BRL REport No. 668, 1948.

(2) Zaroodny, Serge J., and Mott, R. S., Dynamic Measurements On The 81-mm Shell M56 in NBS Wind Tunnel, BRL Report 882, 1953.

(3) Zaroodny, Serge J., Ballistic Analysis of Mortar Shell, BRLM Report 434, 1946.

(4) Zaroodny, Serge J., and Bomberger, Earl E., Spiral Yawing Motions of 81-MM M56 Shell --- A Study in Non-Linear Theory, BRLM Report No. 682, 1953.

(5) Murphy, Charles H., Prediction of the Motion of Missiles Acted on by Non-Linear Forces and Moments, BRL Report No. 995, 1956.

(6) Schmidt, Jo Ann M., A Study of the Resonating Yawing Motion of Asymmetrical Missiles by Means of Analog Computer Simulation BRL Report No. 992, 1954.

(7) GER 5164 Operation and Maintenance of L3 GEDA, 1 June 1953.

(8) Zaroodny, Serge J., Failure of the Instability of Spin of the First Kind, BRLM Report No. 832, 1954.

(9) NACA RM L56G20a CONFIDENTIAL

LIST OF FIGURES

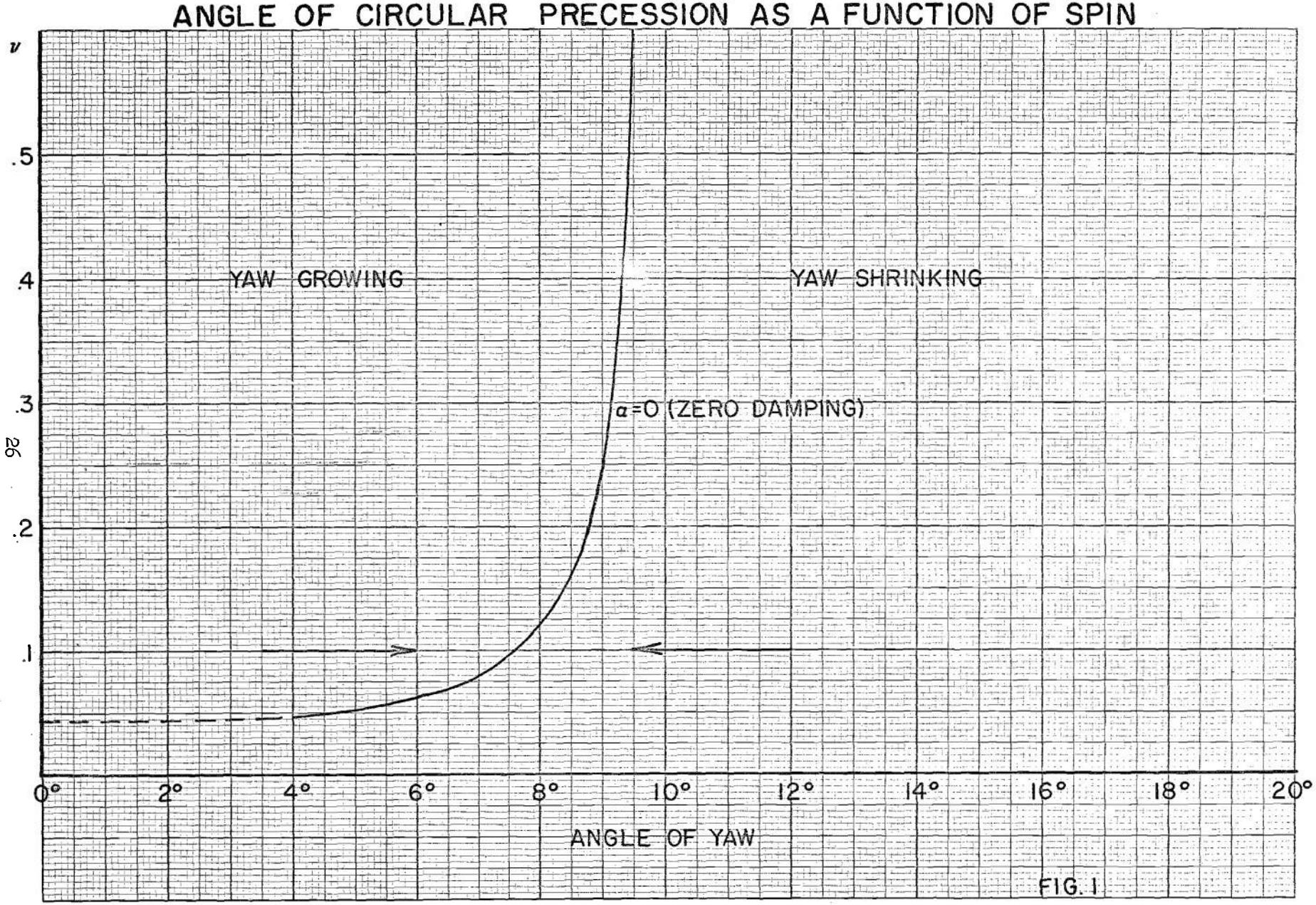
ANGLE OF CIRCULAR PRECESSION AS A FUNCTION OF SPIN
ν
.5
.4
.3
.2
.1
YAW GROWING
YAW SHRINKING
α=0 (ZERO DAMPING)
0°
2°
4°
6°
8°
10°
12°
14°
16°
18°
20°
ANGLE OF YAW

FIG. 1

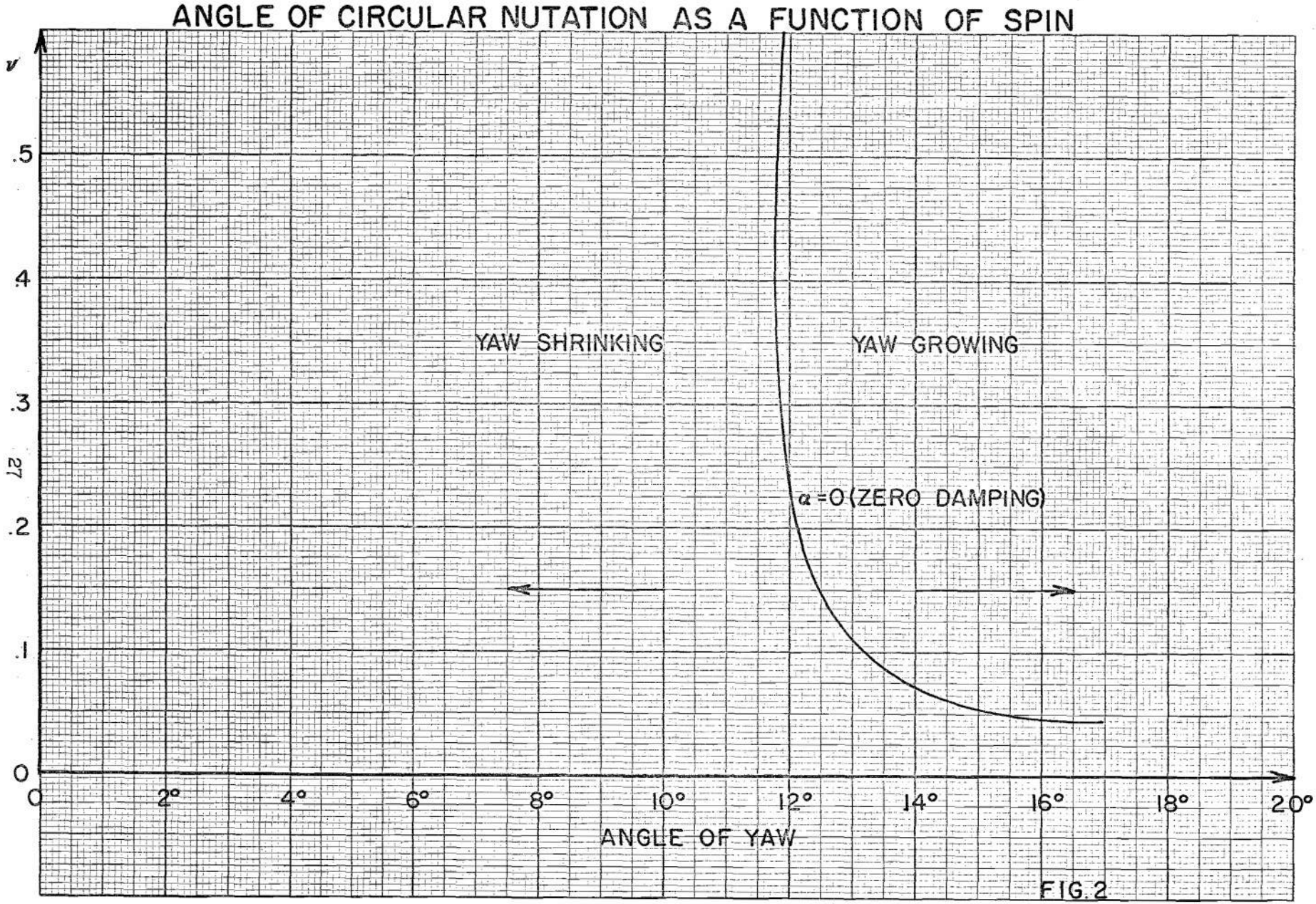
ANGLE OF CIRCULAR NUTATION AS A FUNCTION OF SPIN
v
.5
.4
.3
.2
.1
0
27
YAW SHRINKING
YAW GROWING
α = 0 (ZERO DAMPING)
0
2°
4°
6°
8°
10°
12°
14°
16°
18°
20°
ANGLE OF YAW

FIG. 2

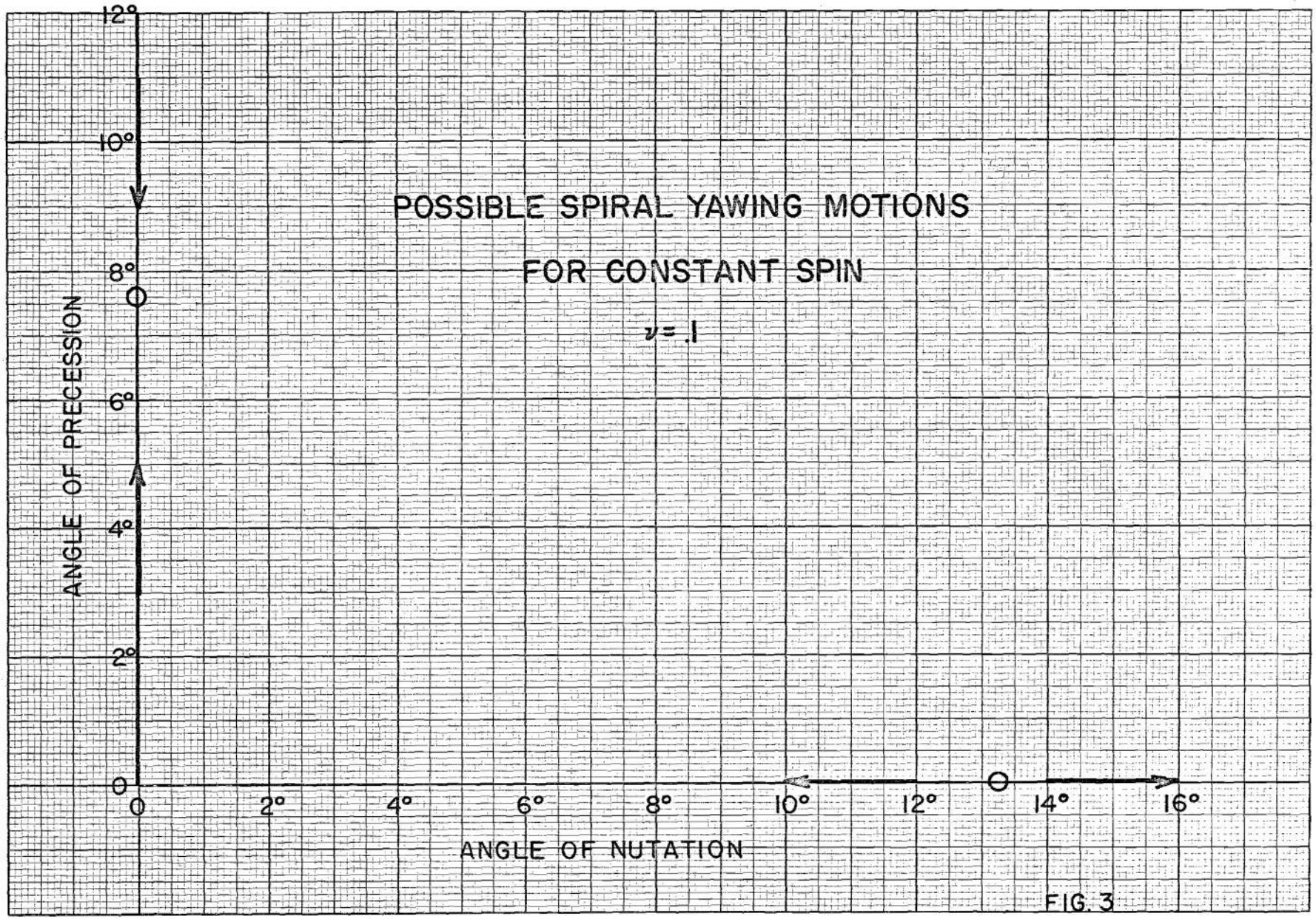
POSSIBLE SPIRAL YAWING MOTIONS
FOR CONSTANT SPIN
$\nu = .1$
ANGLE OF PRECESSION
12°
10°
8°
6°
4°
2°
0
0
2°
4°
6°
8°
10°
12°
14°
16°
ANGLE OF NUTATION

FIG. 3

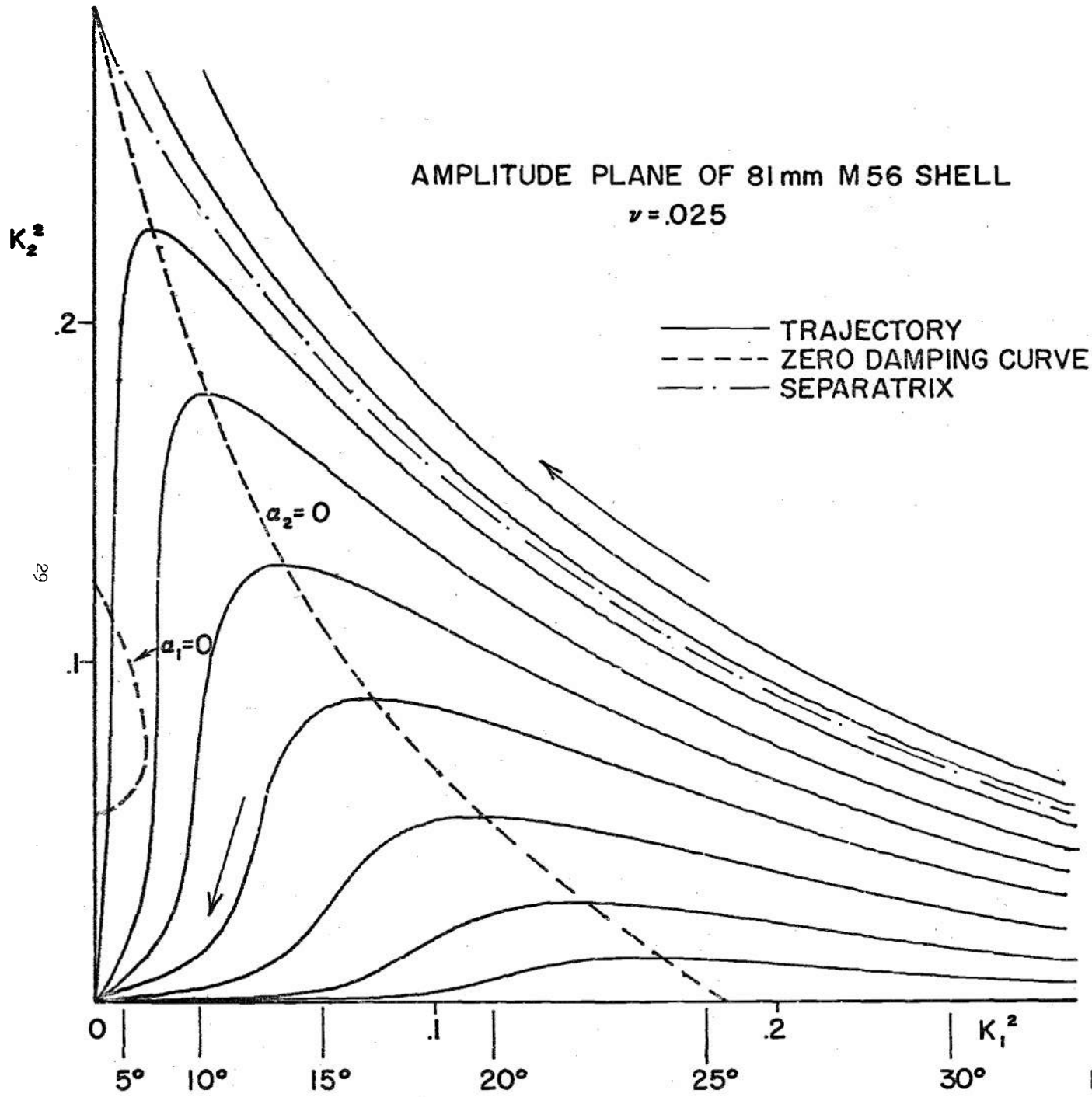
AMPLITUDE PLANE OF 81mm M56 SHELL
ν=.025
TRAJECTORY
ZERO DAMPING CURVE
SEPARATRIX
K_2^2
.2
.1
$a_2=0$
$a_1=0$
0
.1
.2
K_1^2
5°
10°
15°
20°
25°
30°

FIG. 4

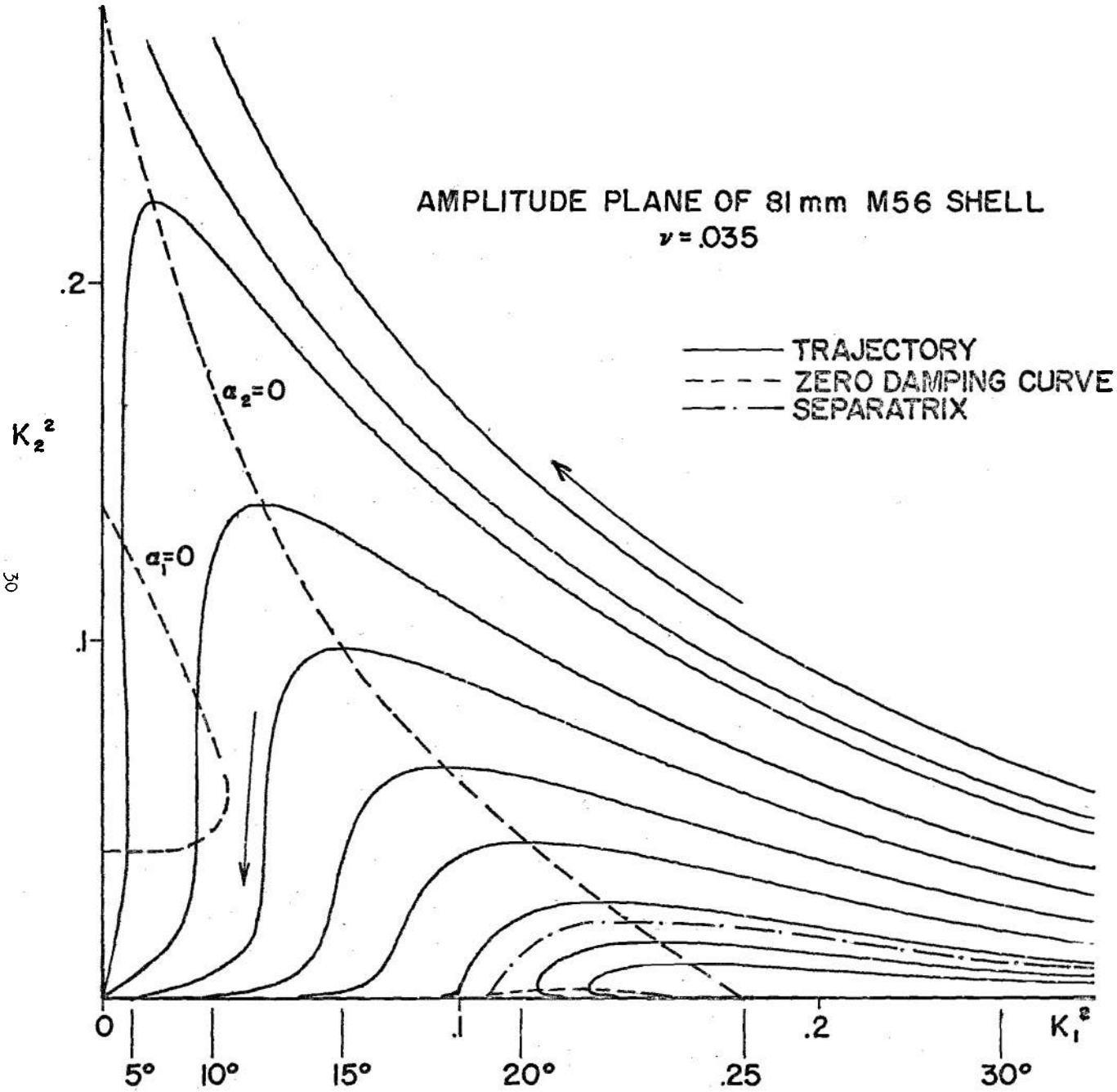
AMPLITUDE PLANE OF 81 mm M56 SHELL
ν = .035
TRAJECTORY
ZERO DAMPING CURVE
SEPARATRIX
K_2^2
K_1^2
$\alpha_2=0$
$\alpha_1=0$
.2
.1
0
.1
.2
.25
5°
10°
15°
20°
30°

FIG.5

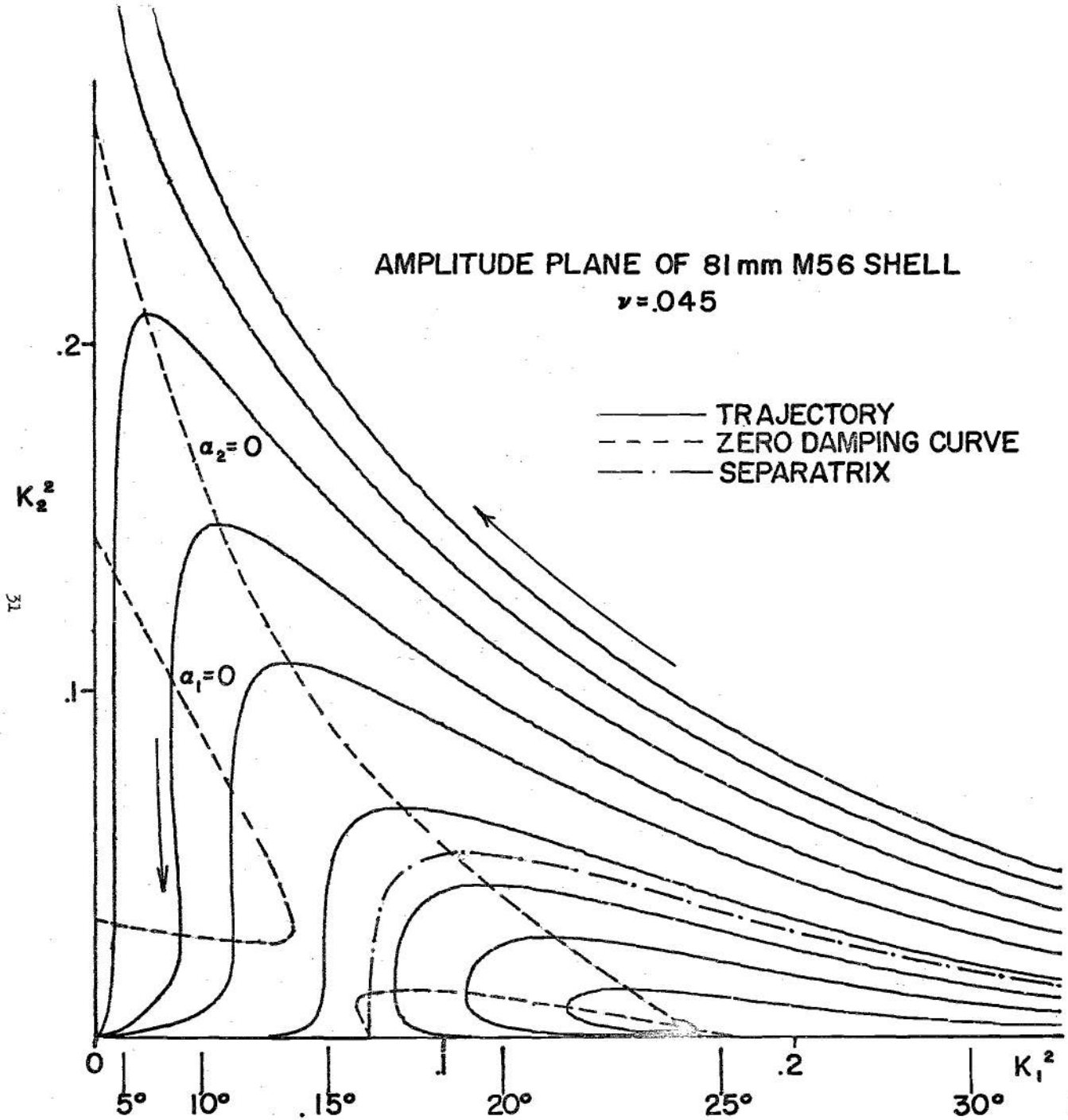
AMPLITUDE PLANE OF 81mm M56 SHELL
ν=.045
TRAJECTORY
ZERO DAMPING CURVE
SEPARATRIX
K_2^2
K_1^2
$\alpha_2=0$
$\alpha_1=0$
.2
.1
0
.1
.2
5°
10°
.15°
20°
25°
30°

FIG. 6

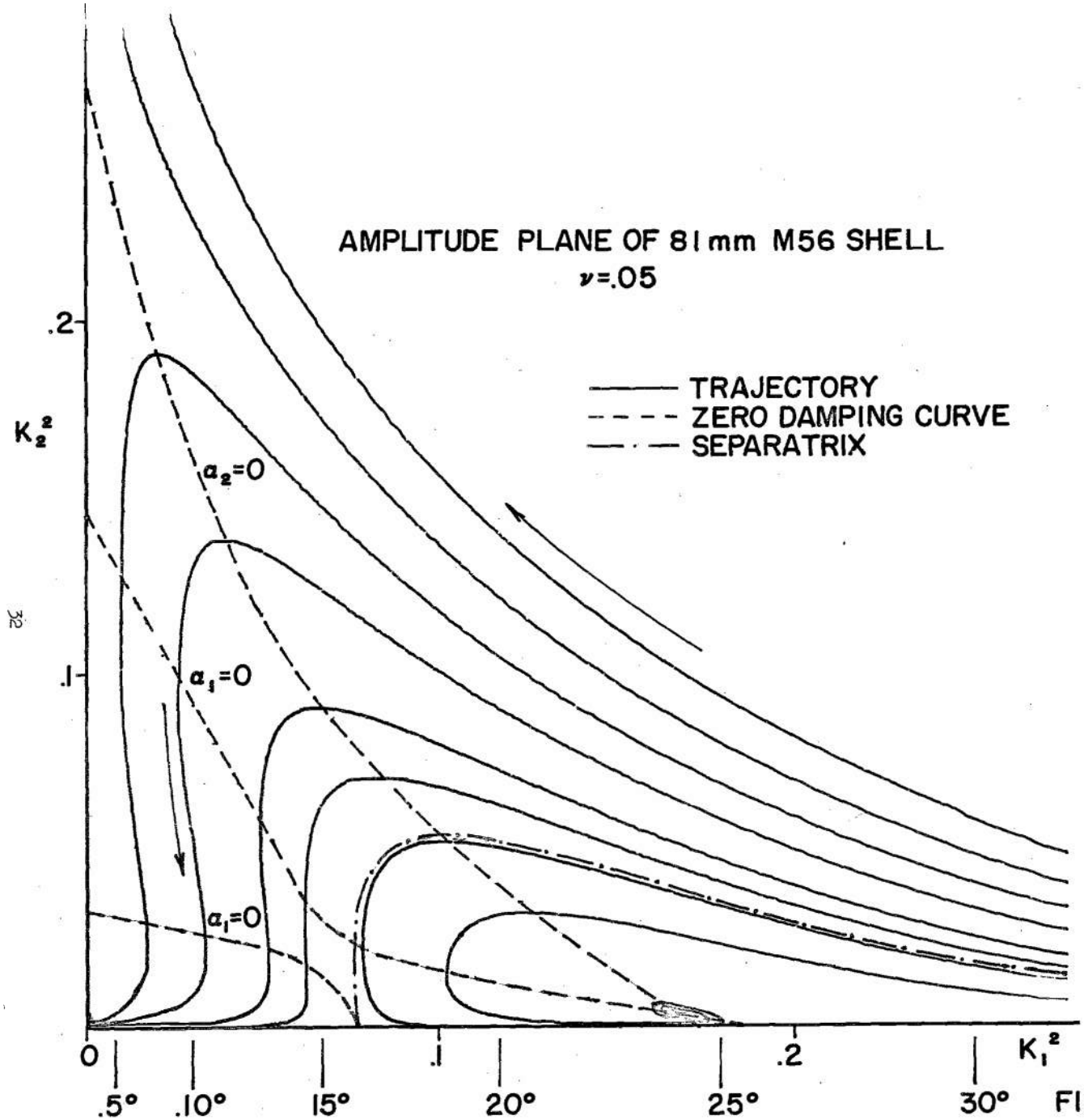
AMPLITUDE PLANE OF 81mm M56 SHELL
ν=.05
TRAJECTORY
ZERO DAMPING CURVE
SEPARATRIX
K₂²
.2
.1
α₂=0
α₁=0
α₁=0
0
.1
.2
K₁²
.5°
.10°
15°
20°
25°
30°

FIG. 7

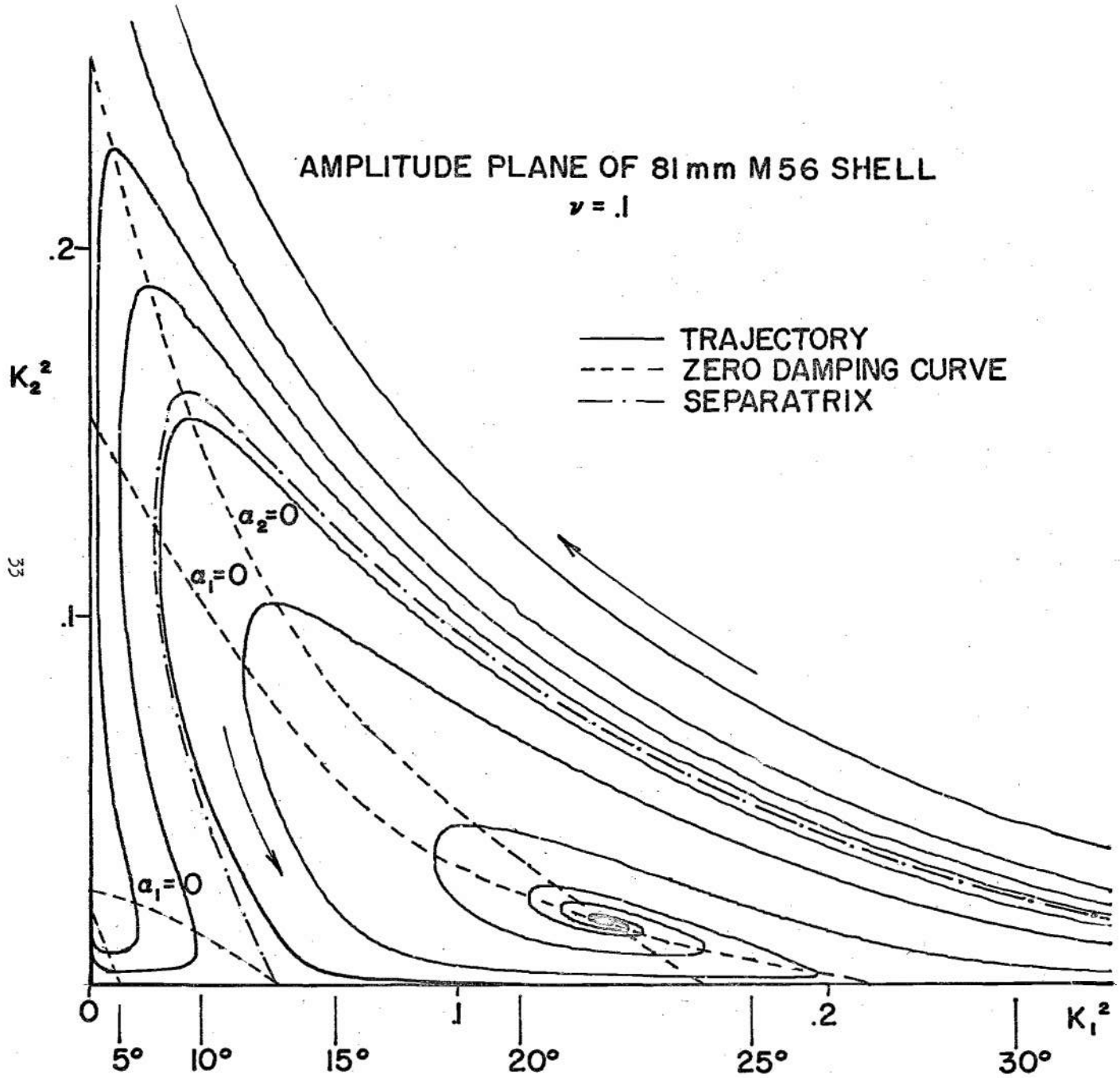
AMPLITUDE PLANE OF 81mm M56 SHELL
ν = .1
TRAJECTORY
ZERO DAMPING CURVE
SEPARATRIX
K_2^2
.2
.1
$\alpha_2=0$
$\alpha_1=0$
$\alpha_1=0$
0
.1
.2
K_1^2
5°
10°
15°
20°
25°
30°

FIG. 8

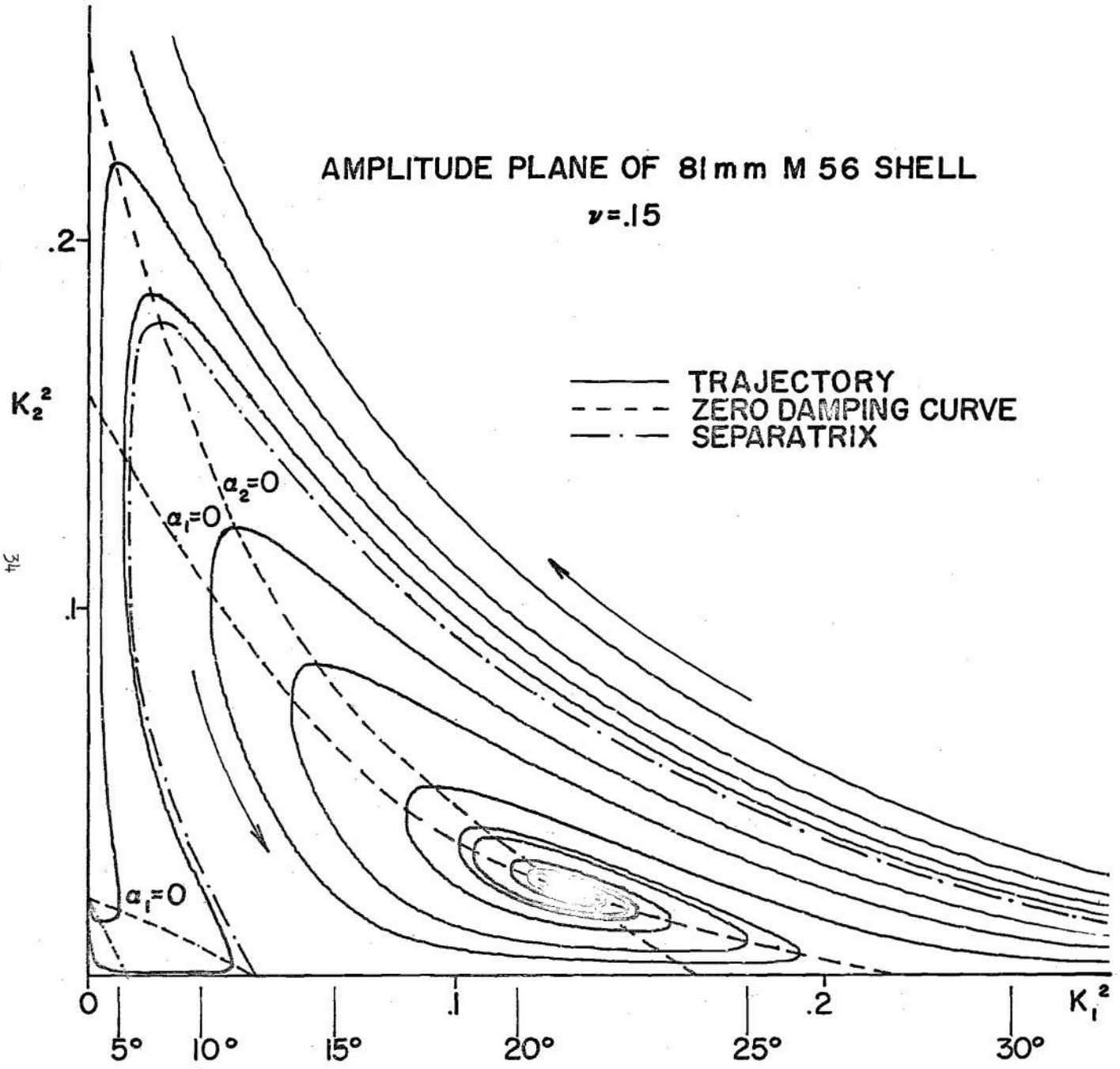
AMPLITUDE PLANE OF 81mm M 56 SHELL
ν=.15
TRAJECTORY
ZERO DAMPING CURVE
SEPARATRIX
K_2^2
K_1^2
$\alpha_2=0$
$\alpha_1=0$
$\alpha_1=0$
.2
.1
0
.1
.2
5°
10°
15°
20°
25°
30°

FIG.9

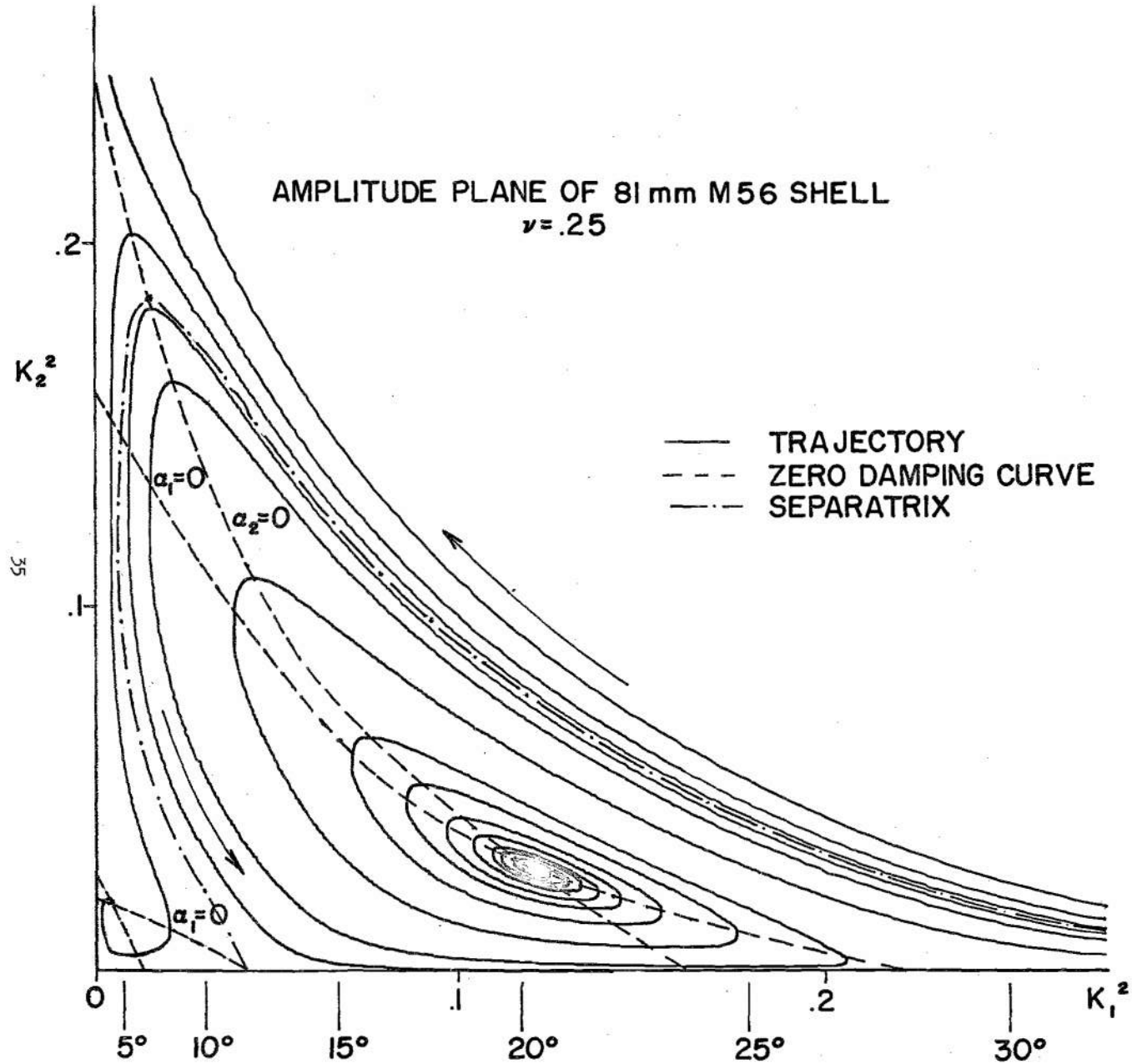
AMPLITUDE PLANE OF 81 mm M56 SHELL
ν = .25
TRAJECTORY
ZERO DAMPING CURVE
SEPARATRIX
K_2^2
K_1^2
$\alpha_1=0$
$\alpha_2=0$
$\alpha_1=0$
.2
.1
0
.1
.2
5°
10°
15°
20°
25°
30°

FIG. 10

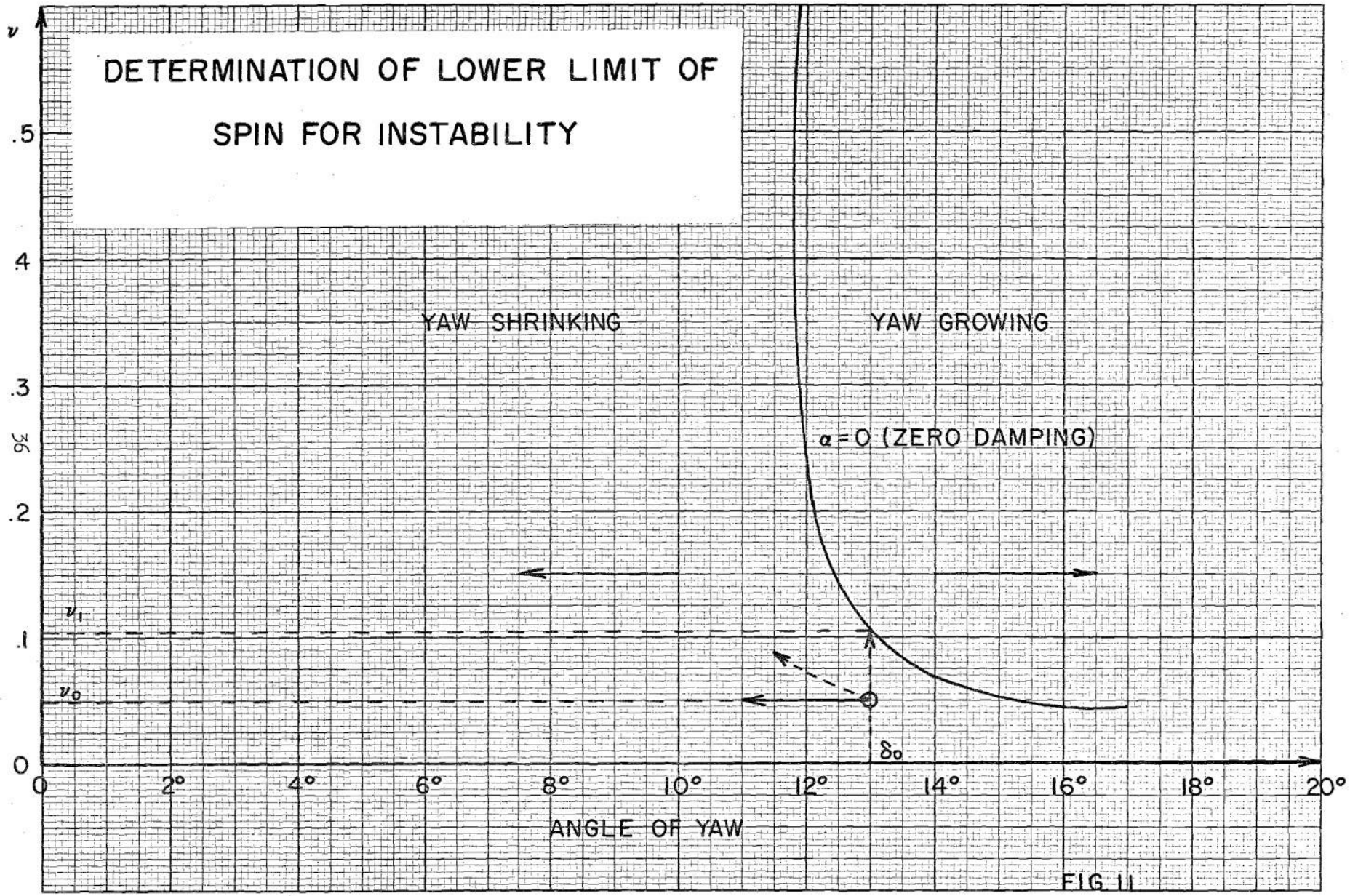
DETERMINATION OF LOWER LIMIT OF SPIN FOR INSTABILITY
ν
.5
.4
.3
.2
.1
0
YAW SHRINKING
YAW GROWING
α = 0 (ZERO DAMPING)
ν1
ν0
δ0
0
2°
4°
6°
8°
10°
12°
14°
16°
18°
20°
ANGLE OF YAW

FIG 11

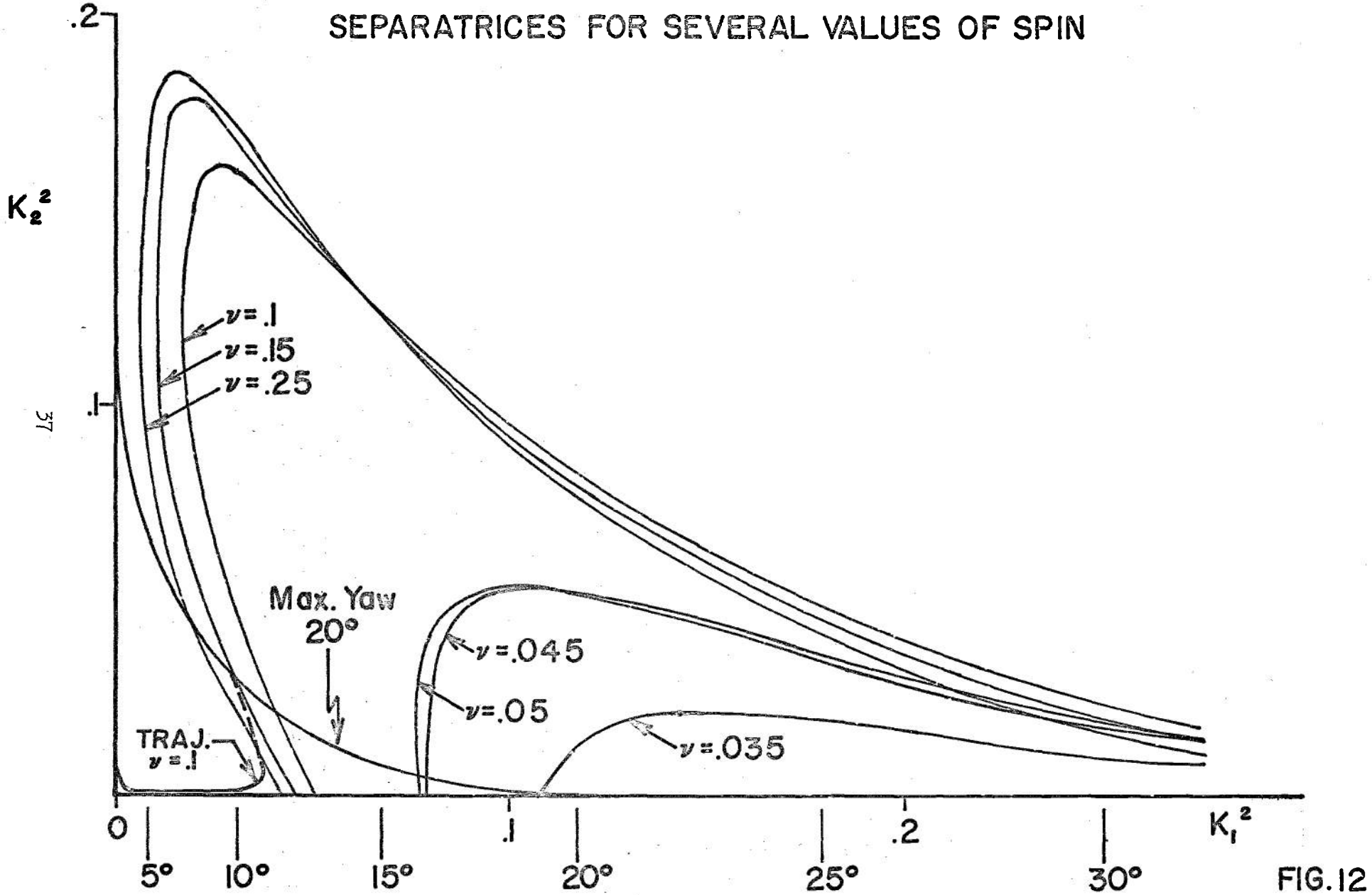
SEPARATRICES FOR SEVERAL VALUES OF SPIN
.2
K_2^2
.1
ν=.1
ν=.15
ν=.25
Max. Yaw
20°
ν=.045
ν=.05
ν=.035
TRAJ.
ν=.1
0
5°
10°
15°
.1
20°
25°
.2
30°
K_1^2

FIG. 12

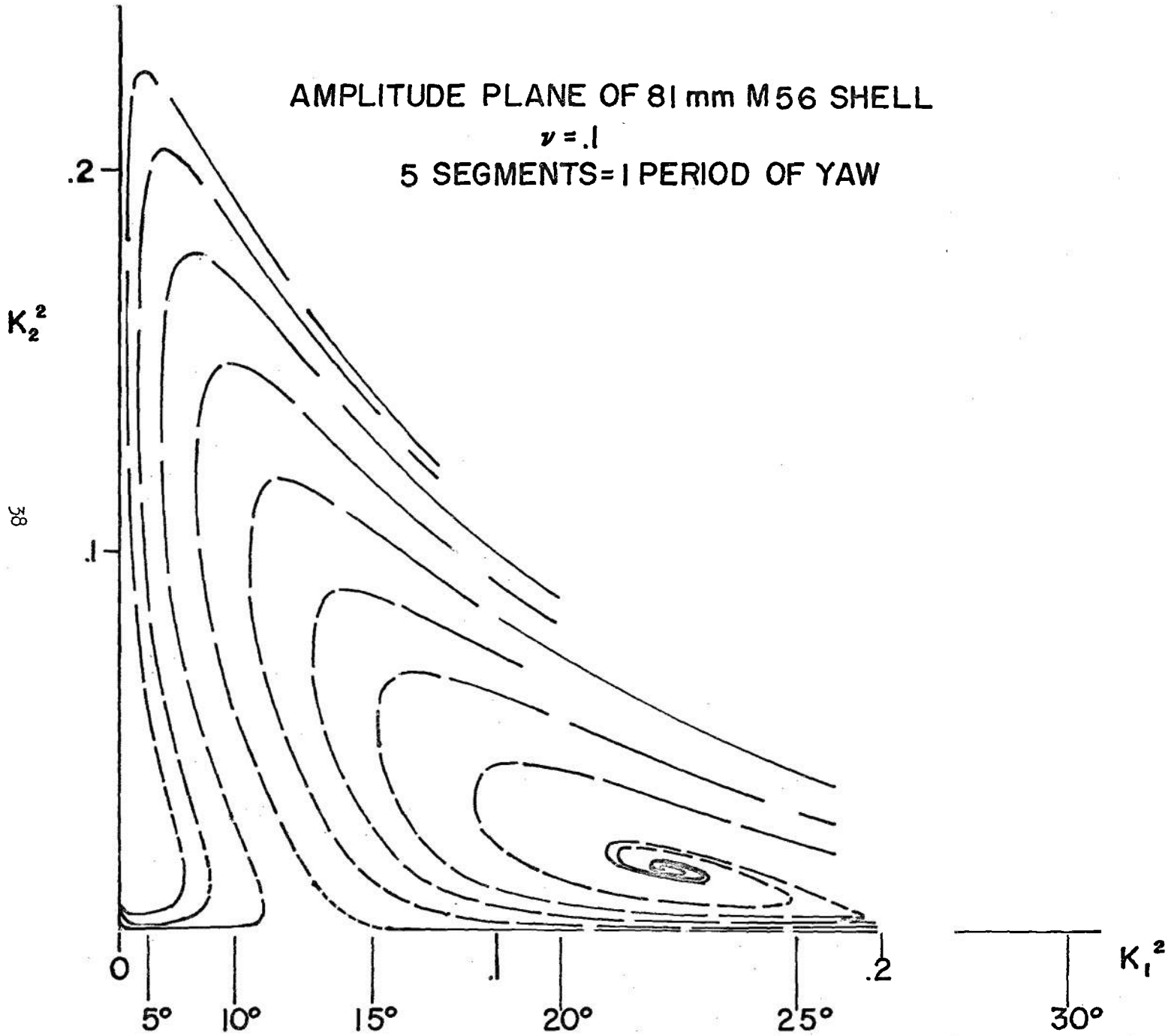
AMPLITUDE PLANE OF 81 mm M56 SHELL
ν = .1
5 SEGMENTS = 1 PERIOD OF YAW
K_2^2
.2
.1
0
.2
K_1^2
5°
10°
15°
20°
25°
30°

FIG. 13

DISTRIBUTION LIST

No. of Copies	Organization
	Chief of Ordnance Department of the Army Washington 25, D. C. Attn: ORDTB - Bal Sec ORDTA ORDTX-AR
10	British Joint Services Mission 1800 K Street, N. W. Washington 6, D. C. Attn: Mr. John Izzard, Reports Officer
4	Canadian Army Staff 2450 Mass. Ave., N. W. Washington 8, D. C.
3	Chief, Bureau of Ordnance Department of the Navy Washington 25, D. C. Attn: ReO
2	Commander Naval Proving Ground Dahlgren, Virginia
2	Commander Naval Ordnance Laboratory White Oak Silver Spring, Maryland Attn: Mr. Nestinger Dr. May
1	Superintendent Naval Postgraduate School Monterey, California
2	Commander Naval Air Missile Test Center Point Mugu, California
1	Commanding Officer and Director David W. Taylor Model Basin Washington 7, D. C. Attn: Aerodynamics Laboratory
1	Commander Naval Air Development Center Johnsville, Pennsylvania
1	Commanding Officer Naval Air Rocket Test Station Lake Denmark Dover, New Jersey
2	Commander Naval Ordnance Test Station China Lake, California Attn: Technical Library
4	Commander Air Research and Development Command P. O. Box 1395 Baltimore 3, Maryland Attn: Deputy for Development
1	Commander Air Force Armament Center Eglin Air Force Base, Florida Attn: ACOT
1	Commander Arnold Engineering Development Center Tullahoma, Tennessee Attn: Deputy Chief of Staff, R&D
10	Director Armed Services Technical Information Agency Documents Service Center Knott Building Dayton 2, Ohio Attn: DSC-SD

DISTRIBUTION LIST

No. of Copies	Orgnaization
2	U. S. Atomic Energy Commission Sandia Corporation P. O. Box 5900 Albuquerque, New Mexico
1	Director National Advisory Committee for Aeronautics 1512 H Street, N. W. Washington 25, D. C.
1	Director National Advisory Committee for Aeronautics Ames Laboratory Moffett Field, California Attn: Dr. A. C. Charters Mr. H. J. Allen
3	National Advisory Committee for Aeronautics Langley Memorial Aeronautical Laboratory Langley Field, Virginia Attn: Mr. J. Bird Mr. E. E. Brown Dr. Adolf Busemann
1	National Advisory Committee for Aeronautics Lewis Flight Propulsion Laboratory Cleveland Airport Cleveland, Ohio Attn: F. K. Moore
1	Director, JPL Ord Corps Installation 4800 Oak Grove Drive Department of the Army Pasadena, California Attn: Mr. Irl E. Newlan, Reports Group

No. of Copies	Organization
1	Commanding General Redstone Arsenal Huntsville, Alabama Attn: Technical Library
3	Commanding Officer Picatinny Arsenal Dover, New Jersey Attn: Samuel Feltman Ammunition Labs.
1	Commanding General Frankford Arsenal Philadelphia 37, Penna. Attn: Reports Group
1	Commanding Officer Chemical Corps Chemical & Radiological Lab. Army Chemical Center, Maryland
1	The Johns Hopkins University Operations Research Office 7100 Connecticut Avenue Chevy Chase, Maryland Washington 15, D. C.
2	Armour Research Foundation Illinois Institute of Technology Technology Center Chicago 16, Illinois Attn: Mr. W. Casier Dr. A. Wundheiler
2	Applied Physics Laboratory 8621 Georgia Avenue Silver Spring, Maryland Attn: Mr. George L. Seielstad

DISTRIBUTION LIST

No. of Copies	Organization
1	Aerophysics Development Corporation P. O. Box 657 Pacific Palisades, Calif. Attn: Dr. William Bollay
1	Cornell Aeronautical Laboratory, Inc. 4455 Genesee Street Buffalo, New York Attn: Miss Elma T. Evans, Librarian
1	CONVAIR Division of General Dynamics Corporation Ordnance Aerophysics Laboratory Daingerfield, Texas Attn: Mr. J. E. Arnold
1	M. W. Kellogg Company Foot of Danforth Avenue Jersey City 3, New Jersey Attn: Miss E. M. Hedley
1	University of Michigan Willow Run Research Center Willow Run Airport Ypsilanti, Michigan Attn: Mr. J. E. Corey
1	University of Southern California Engineering Center Los Angeles 7, Calif. Attn: Mr. H. R. Saffell, Director
1	United Aircraft Corporation Research Department East Hartford 8, Connecticut Attn: Mr. C. H. King
1	Wright Aeronautical Division Curtiss-Wright Corporation Wood-Ridge, New Jersey Attn: Sales Department (Government)
1	Professor George E. Carrier Division of Applied Sciences Harvard University Cambridge 38, Massachusetts
1	Professor Francis H. Clauser, Jr. Department of Aeronautics Johns Hopkins University Baltimore 18, Maryland
1	Professor Clark B. Millikan Guggenheim Aeronautical Laboratory California Institute of Technology Pasadena 4, California
1	Dr. A. E. Puckett Hughes Aircraft Company Culver City, California
1	Dr. L. H. Thomas Watson Scientific Computing Laboratory 612 West 116th Street New York 27, New York

Army--Aberdeen Proving Ground, Md--D